Impact of warmer sea surface temperature on the global pattern of intense convection: insights from a global storm resolving model

Kai-Yuan Cheng[1,2], Lucas Harris[2], Christopher Bretherton[3], Timothy Merlis[1], Maximilien Bolot[1], Linjiong Zhou[1,2], Alex Kaltenbaugh[2,4], Spencer Clark[2,3], and Stephan Fueglistaler[1]

[1]Program in Oceanic and Atmospheric Sciences, Princeton University, Princeton, NJ, USA.

[2]NOAA/Geophysical Fluid Dynamics Laboratory, Princeton, NJ, USA.

[3]Allen Institute for Artificial Intelligence, Seattle, WA, USA.

[4]University Corporation for Atmospheric Research, Boulder, CO, USA.

Corresponding author: Kai-Yuan Cheng (kai-yuan.cheng@noaa.gov)

Key Points:

- A global storm resolving model is used to conduct year-long simulations to study the change of intense convection in a warmed climate
- Increased SST modulates the frequency of intense convection with large spatial and seasonal variations
- Increases in convective available potential energy do not necessarily enhance intense convection frequency

Abstract

Intense convection (updrafts exceeding 10 $m \cdot s^{-1}$) plays an essential role in severe weather and Earth's energy balance. Despite its importance, how the global pattern of intense convection changes in response to warmed climates remains unclear, as simulations from traditional climate models are too coarse to simulate intense convection. Here we take advantage of a kilometer-scale global storm resolving model and conduct year-long simulations of a control run, forced by analyzed sea surface temperature (SST), and one with a 4-K increase in SST for comparison. Comparisons show that the increased SST enhances the frequency of intense convection globally with large spatial and seasonal variations. Increases in the intense convection frequency do not necessarily reflect increases in convective available potential energy (CAPE). Results are also compared with traditional climate model projections. Changes in the spatial pattern of intense convection are associated with changes in planetary circulation.

Plain Language Summary

Intense convection, which we sense as strong thunderstorms, is a major cause of damaging weather and an important component in Earth's energy balance. However, it is still unclear how intense convection changes in a warmed climate because traditional climate models cannot resolve these convective events. In order to investigate the impact of a warmed climate on intense convection, we use a new ultra-high-resolution global model to conduct year-long simulations under normal and warmed-ocean conditions. We find that intense convection becomes more frequent globally in a warmed climate. However, some regions have less intense convection. Spatial and seasonal responses of intense convection are associated with the changed planetary circulation. We also find that increases in convective available potential energy do not necessarily favor the development of intense convection.

1 Introduction

Intense convection, featuring large vertical motions and water phase changes, has profound consequences for many aspects of atmospheric and climate science. Intense convection is a major source of weather hazards due to its association with heavy rain, damaging winds, and large hail. Worldwide, the economic loss related to intense convection is about 108 million US

dollars on average every day from 1970 to 2019 (WMO, 2021). In the context of climate, intense convection plays a critical role in Earth's energy balance, as intense convection modulates radiative balance through its effect on both the incoming solar radiation and the outgoing longwave radiation. Furthermore, intense convection modulates energy transfer dynamically and thermodynamically within the atmosphere.

Previous modeling studies (e.g., Diffenbaugh et al., 2013) argued that a warming climate is likely to enhance the frequency and intensity of intense convection. The argument, however, is based on the analysis of convective environmental proxies (e.g., low-level wind shear and CAPE), rather than the simulation of the convection itself. This limitation arises because traditional climate models have too coarse a grid to simulate intense convection explicitly.

This study overcomes this limitation using a global storm-resolving model (GSRM). GSRMs are a new class of global atmosphere models with 2-5 km horizontal resolution that can resolve individual convective storms (Stevens et al., 2019; Satoh et al., 2019). We are unaware of any published GSRM simulations of warming climates, except for the paper done by Tsushima et al. (2014), which investigated the impact of warmer SSTs on high clouds. The resolution of their simulations (7 and 14 km) is insufficient to accurately simulate intense convection, and the simulation periods used (at most 90 days) do not cover the full annual cycle.

In this study, we use a GSRM to explore the impact of global warming on the global distribution of intense convection. We compare two sets of year-long GSRM simulations, a control run and that with 4-K warmer SST, made using the eXperimental System for High-resolution prediction on Earth-to-Local Domains (X-SHiELD) developed at the Geophysical Fluid Dynamics Laboratory (GFDL). X-SHiELD is designed to explicitly resolve convection at scales of 3 km. X-SHiELD has been a part of the Dynamics of the Atmospheric general circulation Modeled On Non-hydrostatic Domains (DYAMOND) project (Stevens et al., 2019) from the project's inception and has been evaluated for tropical cyclones (Judt et al., 2021) and tropical cirrus (Nugent et al., 2021 and Turbeville et al., 2021). The 4-K warmer SST experiment is analogous to the amip4K experiments included in the Coupled Model Intercomparison Project phase 5 (CMIP5; Taylor et al. 2012) and phase 6 (CMIP6; Eyring et al. 2016). X-SHiELD's year-long simulations are unique datasets that allow us to examine the behavior of intense convection in a warming climate.

2 Global storm-resolving model X-SHiELD and experiment design

X-SHiELD, a configuration of a unified modeling system SHiELD (Harris et al., 2020), is a full physics global model powered by the Finite-Volume Cubed-Sphere Dynamical Core (FV^3; Putman & Lin, 2007; Harris et al., 2021). The horizontal resolution of X-SHiELD is ~3.25 km globally. X-SHiELD uses 79 vertical levels where the resolution is the finest (~20 m) at the bottom and gradually expands upward, with a model top at 3 hPa. The physical parameterizations used in X-SHiELD include the in-line GFDL microphysics scheme (Harris et al., 2020; Zhou et al. 2022), the turbulent kinetic energy (TKE)-based moist eddy-diffusivity mass-flux (EDMF) PBL scheme (Han and Bretherton, 2019), the scale-aware simplified Arakawa–Schubert scheme (Han et al., 2017) for shallow convection only, and the Noah-MP land surface model (Niu et al., 2011). A mixed-layer ocean model (Pollard et al., 1973) is used and nudged towards real-time ECMWF SST analyses. The deep convective parameterization is disabled as X-SHiELD explicitly simulates deep convection.

This study aims to investigate how warmer SST affects the development of intense convection. For the purpose of comparison, a control experiment and that with a 4-K warmer SST (4-K hereafter) were conducted. Both experiments use the same model with the same configuration. The only difference in the 4-K experiment is that the SST is nudged towards analyses with a uniform 4 K increase in SST. Both runs are 15 months long starting at 00 UTC on 20 October 2019, and the period from Dec 2019 to Nov 2020 is used for the analysis presented here.

3 Global picture of intense convection

The global annual-mean distribution of intense convection, defined as w_{max} (6-hr column-maximum vertical velocity below 100 hPa) > 10 $m \cdot s^{-1}$, produced by the 4-K and the control experiments are shown in Figure 1a and 1b respectively. Both experiments share a similar pattern consistent with the observed global picture of deep convection (e.g., Houze et al., 2015; Liu et al., 2007), suggesting that X-SHiELD realistically simulates intense convection. Overall, the annual occurrence of intense convection increases by 21% due to the increased SST, which is

also revealed in Figure 1d. In addition to the increased occurrence, the most extreme vertical velocities increase by about 20% in the 4-K run (Figure 1d). The enhancement of convective vertical velocities by the increased SST is consistent with prior theoretical work by Singh & O'Gorman (2015).

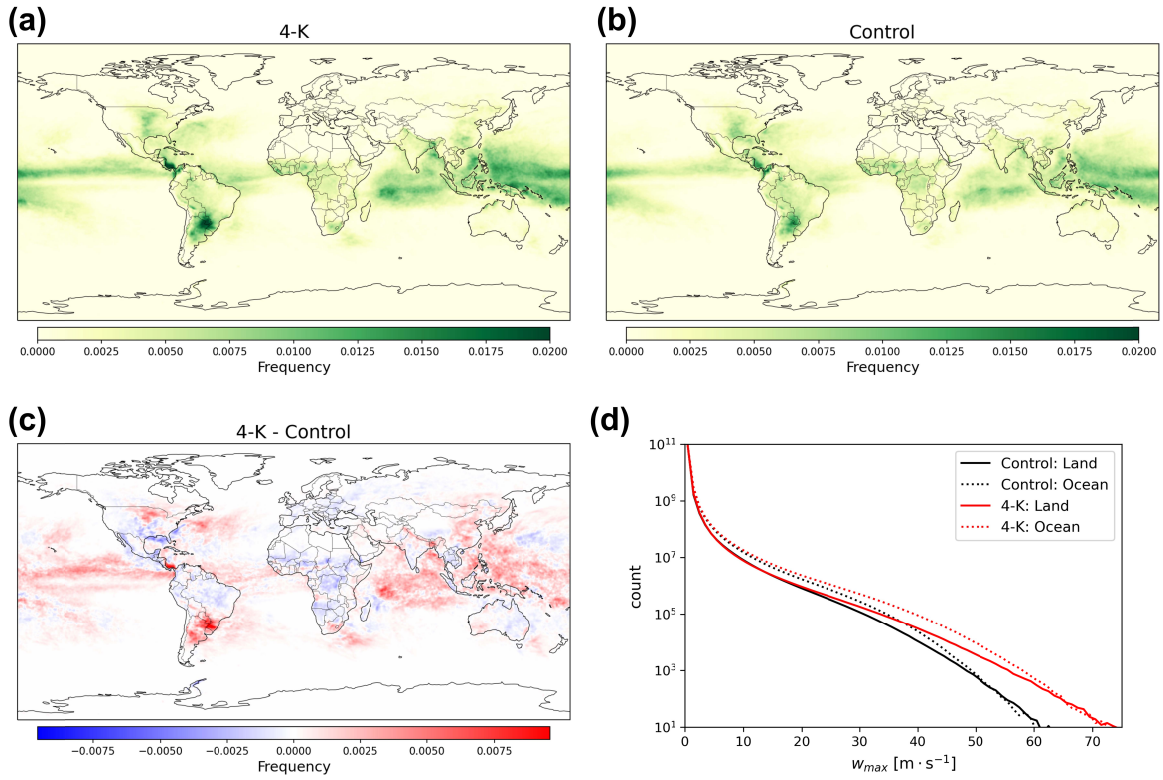

Figure 1. Annual column-maximum vertical velocity occurrence. Global distribution of annual frequencies for (a) 4-K and (b) Control when $w_{max} > 10$ m·s^{-1}. (c) Difference between 4-K and Control. (d) Histogram of w_{max} over the ocean vs. over the land.

The difference between the two experiments (Figure 1c) indicates that in the 4-K run, the ocean becomes more favorable for intense convection, which can be also seen clearly in Figure 1d. For the same vertical velocity, the 4-K run always has a larger frequency difference between the land and the ocean than the control run does, except in the poorly sampled high-w_{max} tail.

Over land, the impact of the increased SST on the frequency of intense convection varies between regions. Figure 1c shows that significant increases are simulated in the northern Midwest of the US, the Argentinian Rio de la Plata basin, Bangladesh, northern India, and eastern China. In contrast, significant decreases are observed in the southeastern US, Amazon

basin, west Eurasia, Congo Basin, and South Asia. These regional differences are associated with the planetary-scale circulation response to the warmed SST, which will be discussed later.

Note that no CO2 increase has been imposed in the 4-K experiment. The lack of a CO2 direct radiative effect may be responsible for the shift of intense convection occurrence from the land to the ocean as shown in Figure 1c and 1d. A realistic corresponding CO2 increase would enhance surface longwave cooling, reduce the sea-land temperature contrast, and move intense convection back over land. We plan to explore these effects using simulations with perturbed CO2 in the near future.

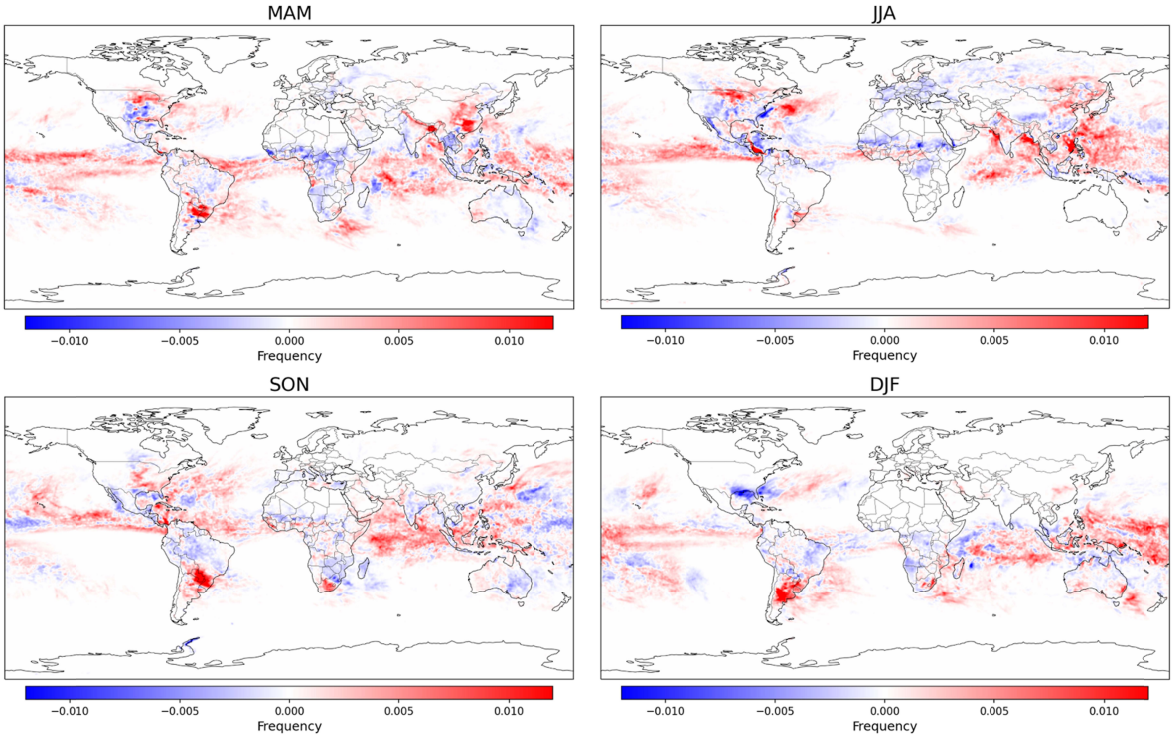

Figure 2. Difference between 4-K and Control frequency of intense convection for individual seasons as indicated by the titles.

Figure 2 shows the seasonal distribution of the difference in intense convection frequency between the two experiments. Intense convection frequencies over the ocean in the 4-K run increase significantly in all seasons, showing that the warmer SST enhances intense convection development over the ocean, which is consistent with the annual difference shown in Figure 1c. The seasonality reflects the climatological shift of the Intertropical Convergence Zone (ITCZ) and the variability of warm currents. With respect to the land, in contrast, the seasonal variability

can be generalized in terms of the warm season and the cold season. The warm season is defined as the period between March-August in the North Hemisphere (NH) and September-December in the South Hemisphere (SH). The cold season refers to the rest of the year for each hemisphere. During the warm season, intense convection tends to develop frequently and the difference between the two runs becomes significant and complex, especially in the NH (SH) during JJA (DJF). Generally, there are increases at high latitudes and decreases at low latitudes in North America, South America, and East Asia, suggesting the increased SST shifts intense convection development to higher latitudes in those regions. In addition, reductions in the frequencies can be seen in west Eurasia and central Africa, suggesting that the increased SST suppresses intense convection development there. For the cold season, on the contrary, the development of convection becomes less active and migrates to lower latitudes. Also, the difference between the two experiments becomes less discernible, which can be depicted clearly in the NH (SH) during DJF (JJA). It shows that the increased SST has a weak impact on the nature of intense convection during the cold season. Exceptions, however, exist. For example, we observe significant reductions taking place in the South of the US during DJF and increases taking place in the Rio de la Plata Basin during JJA. These exceptions suggest that the increased SST suppresses (enhances) intense convection development over the southern US (Rio de la Plata basin).

Lepore et al. (2021) studied how convective severe weather activities change in warmer climates for different seasons, based on analyzing environmental proxies of convection in the CMIP6 ensemble. They found that the frequency of severe weather activities increases globally as the global temperature increases, with higher latitudes showing larger relative changes. Their findings are broadly consistent with our results. However, significant discrepancies exist in many regions and vary seasonally (cf. Figure 7 in Lepore et al., 2021). For example, our simulations show decreases in Europe and the southern US during the warm season, whereas their results show increases in those regions. We note, however, that the frequency of severe weather activities computed by Lepore et al. (2021) is based on convective environmental proxies, not convection itself, as CMIP6 models do not resolve convection. Also, the shift of convection development from the land to the ocean in our 4-K run may partially account for the discrepancies. Moreover, the discrepancies may result from the relatively short simulation periods used by our model, compared to multi-decadal simulations conducted by the CMIP

models. The spatial and seasonal response of intense convection to the increased SST can be affected by the internal variability in our year-long simulations.

Previous global modeling studies on changed climates could not resolve deep convection. Thus we also calculated other convection-related fields, including CAPE, precipitation, 500 hPa vertical pressure velocity ω_{500}, and global mean radiative feedback. This helps put the warming-induced changes in intense convection in a broader physical context. Figure 3a shows that the increased SST enhances CAPE throughout the warmer oceans, and to a lesser extent, over convectively-active land regions. This distribution of CAPE change in our model qualitatively agrees with climate model projections (Chen et al., 2020; Fasullo, 2012, Sobel & Camargo, 2011). Quantitatively, the overall increase of CAPE in the tropics is over 300 $J \cdot kg^{-1}$, or over 40% with respect to the control run, which is much higher than the CAPE calculated by traditional climate models for warming climates.

We also compare our results with observations. Taszarek et al. (2021) calculated trends in CAPE under global warming based on ERA5 reanalysis and rawinsonde observations. Our results qualitatively agree with the observations, but not with ERA5. Both their observations and our model analysis show a warming climate enhances CAPE in the Midwest of the US, Rio de la Plata basin, and East China. Both also show reduced CAPE in parts of west Europe. On the other hand, our result does not agree with the trends calculated by the ERA5 reanalysis, which shows CAPE increases over western Europe and decreases over East China, Rio de la Plata basin and over the ocean. The pattern of CAPE changes due to the increased SST generally resembles that of intense convection frequency shown in Figure 1c. However, discrepancies can be observed in regions, such as South Africa and Congo basin, where enhanced CAPE does not necessarily increase intense convection frequencies. In fact, intense convection frequencies may even decrease in regions with increased CAPE, e.g., Amazon Basin. It shows that analyzing convective environmental proxies is insufficient to understand the global picture of intense convection and that GSRMs are a useful tool for the study of intense convection on a global scale.

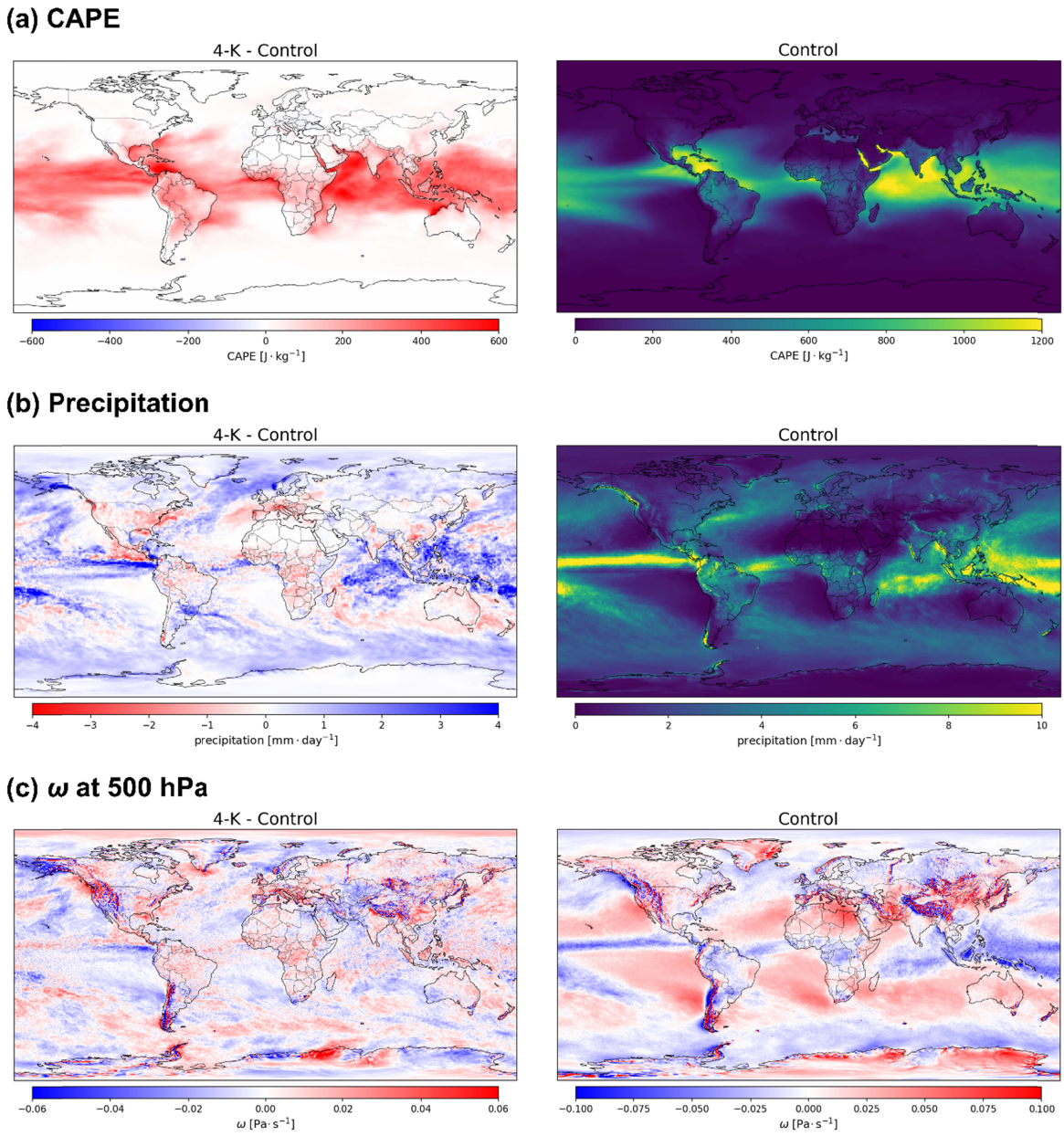

Figure 3. (left) Annual change (4-K - Control) and (right) annual distribution from the control run for CAPE, precipitation, and ω_{500}.

The change in mean precipitation due to the increased SST is shown in Figure 3b. The pattern of the change is similar to the change in intense convection frequency (Figure 1c) in the tropics and subtropics, where most precipitation is associated with deep convection. There are substantial increases over the tropical oceans and little increases over most tropical land. Discrepancies can be observed in the extratropics, where a large fraction of precipitation is not

produced by deep convection. Precipitation significantly increases over the ocean, while the change in the intense convection frequency is tiny.

The pattern of the precipitation change generally agrees with the multimodel mean of the corresponding uniform SST warming CMIP5 experiment (He et al. 2014) and the results of Zhao (2021), who used a 50-km climate model to investigate the change in precipitation in a warmed climate that is forced by a uniform 4 K increase in SST (cf. Figure 9 in Zhao, 2021). Zhao (2021) found that the precipitation changes in tropics and subtropics are associated with tropical storms and mesoscale convection systems, consistent with our results. The changes in extratropics are associated with atmospheric rivers.

In low latitudes, deep convection (which generates latent heating) is tightly connected to vertical motion, as can be seen by comparing Figure 3b (control-climate precipitation) with Figure 3c (control-climate ω_{500}). The change in ω_{500} due to increased SST is generally in the opposite sense as the change in precipitation, with regions of increased ascent (negative change in ω_{500}) coinciding with increased precipitation. The pattern is consistent with previous studies on how the tropical circulation changes under global warming (e.g., Vecchi and Soden, 2007; Wyant et al. 2006). Vecchi and Soden (2007) found that the ω_{500} change opposes the background ω_{500} in tropics and subtropics, indicating a weakening of the mean tropical circulation as can be also seen in our simulations. The result suggests that the robustly simulated weakening of the tropical circulation in a warmed climate holds in this year-long GSRM, notwithstanding the increase in intense convection frequency.

Intense convective clouds and associated tropical cirrus are also an important contributor to the global radiation budget and its changes in a warmer climate. Ringer et al. (2014) found that the change in global cloud radiative effect is highly correlated between GCM simulations forced with a uniform 4 K SST increase and fully-coupled simulations of the climate response to CO2 quadrupling, even though the detailed spatial patterns of cloud change are less similar. The changes in global annual average all-sky top-of-atmosphere longwave and shortwave radiation are -1.66 and 0.06 $W \cdot m^{-2} K^{-1}$, respectively, for a net radiative feedback of -1.6 $W \cdot m^{-2} K^{-1}$, which is squarely within the GCM interquartile range shown for amip4K results in Figure 1 of Ringer et al. (2014). This is based on a global average surface air temperature increase of 4.3 K between

237 our control and 4-K simulations. We conclude that the radiative response of X-SHiELD to SST
238 warming is broadly similar to that of current GCMs.

239

240 **4 Changed planetary-scale circulation and its impact on intense convection development**

241 We have shown changes in the spatial and seasonal variability of intense convection in a
242 warmer climate due to increased SST. One important question then arises: how are such changes
243 coupled to planetary-scale circulation features? Beyond examining the mean vertical velocity, it
244 is helpful to examine how the planetary-scale circulation changes in response to the increased
245 SST, which may provide clues for the change in the intense convection pattern.

246 We use eddy geopotential height (*He*) to depict the impact of the increased SST on
247 subtropical highs, as shown in Figure 4. *He* has been used extensively in examining the nature of
248 the Western North Pacific Subtropical High (see He et al., 2015 and Zhou et al., 2009). *He* is
249 defined as the deviation of the geopotential height at 500 hPa from the regional average over the
250 tropics and subtropics. so it is suitable for the comparison of the pressure patterns between a
251 warmed climate and a normal climate.

252 We first consider the NH. Compared to the control run, the subtropical high over North
253 America in the 4-K run becomes stronger and expands northward and eastward, covering most of
254 the continental United States. This helps suppress intense convection in that simulation. High
255 pressure also expands northward over West Africa. This could partially explain the decrease in
256 the intense convection frequency over west Eurasia. In contrast, the Western North Pacific
257 Subtropical High weakens a bit in the 4-K run, which may explain the increased intense
258 convection frequency over East China during the warm season. In the SH the subtropical highs
259 are strengthened by the increased SST. This reduces the intense convection frequency in
260 subtropical regions of South America, South Africa, and Australia during the warm season.

261 The changed circulation also affects low-level heat and moisture fluxes regionally,
262 which, in turn, modulates intense convection. For example, the intensified circulation around the
263 Bermuda High brings more warm and moist air to the Midwest of the US, enhancing intense
264 convection frequency there. These circulation changes are in part nonlocally driven by latent
265 heating from deep convection and would be altered if CO2 changes were also included in these

simulations. The interaction between intense convection and planetary-scale circulation is a subject for which GSRM simulations are particularly attractive since they can explicitly simulate both processes.

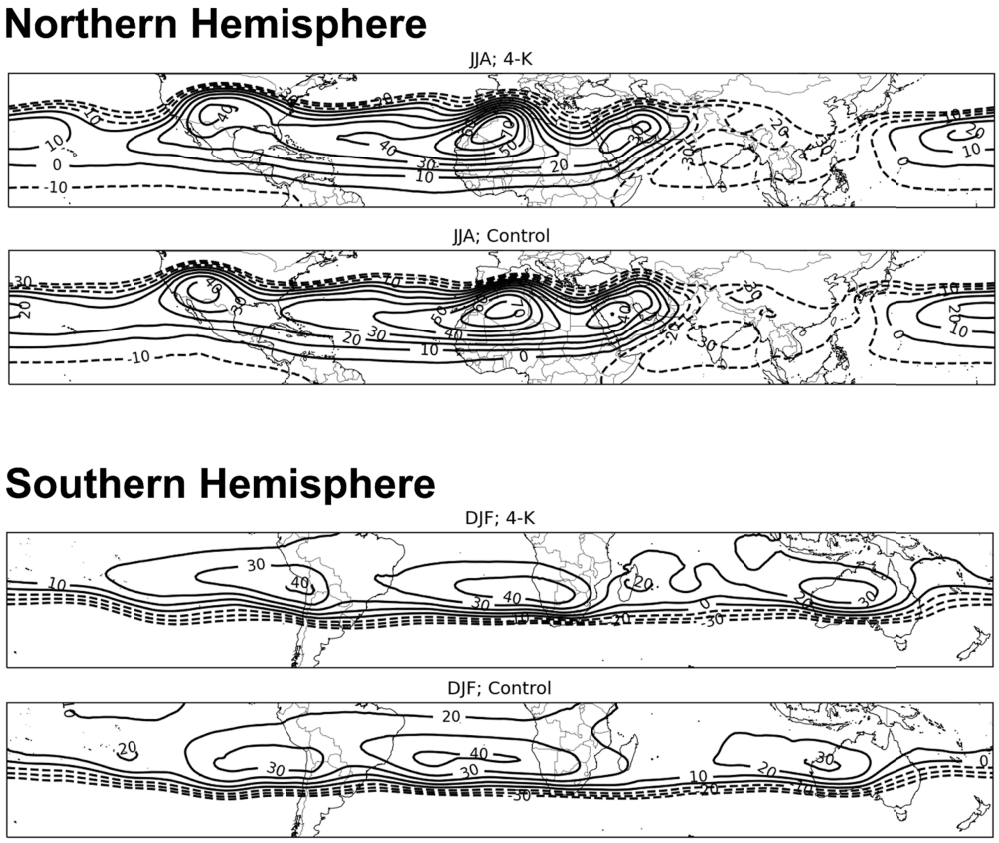

Figure 4. Eddy component of the 500 hPa geopotential height in summer for both 4-K and control experiments. Top two rows: Northern Hemisphere during JJA. Bottom two rows: Southern Hemisphere during DJF. Negative contours are dashed.

5 Conclusions

We have demonstrated that X-SHiELD, a GSRM, is a useful tool for research of intense convection (with updrafts exceeding 10 $m \cdot s^{-1}$) on a global scale. To study the impact of global warming on the global picture of intense convection, two X-SHiELD year-long simulations, control vs. 4-K warmer SST, were compared. The control simulation gives a realistic annual and seasonal distribution of intense convection globally. Increased SST enhances intense convection

throughout the warm oceans where deep convection is common. During the warm season, the increased SST tends to shift intense convection over land to higher latitudes in North America, South America, and East Asia. The increased SST, however, reduces the intense convection frequencies in west Eurasia and central Africa. During the cold season, the increased SST reduces intense convection in the southern US but enhances it in the Rio de la Plata basin.

We compared aspects of our novel year-long global storm-resolving simulations that are connected to intense convection with climate models and observational analyses documented in previous studies. CAPE, precipitation, and ω_{500} were examined, as the global survey of intense convection frequency is unavailable in previous studies. The change in CAPE due to the increased SST shares a similar pattern as seen in previous studies, albeit our simulations give a much larger increase in CAPE over the tropical ocean. In some land regions, increased CAPE does not necessarily correlate with more intense convection. For precipitation and ω_{500}, their changes due to the increased SST in X-SHiELD are consistent with previous studies. We found that the radiative response of X-SHiELD to the increased SST is also similar to that of current GCMs. This gives us confidence that our X-SHiELD findings about the distribution and causes of intense deep convection in a changing climate can inform the future development of GCMs.

We also showed that the increased SST modulates the planetary-scale circulation and, in turn, affects the global pattern of intense convection. The increased SST enhances subtropical highs and drives the poleward shift of intense convection development. The changed circulation also modulates low-level heat and moisture fluxes regionally and in turn the distribution of intense convection.

One caveat of this study is that the simulated seasonality (e.g., intense convection and *He*) is subject to the internal variability of one-year-long simulations, which may partially account for the discrepancies between our simulations and the multi-year mean results from previous studies. We also reiterate that warmer SST is only a partial proxy for a warmer climate because radiative changes from CO2 and horizontal variations in the SST increase driven by ocean coupling are also important. While global-scale changes in convection and circulation due to the increased SST should be robust, these factors will change the warming-induced spatial patterns of convection and circulation. We plan to conduct CO2-forced experiments for direct comparison shortly.

Acknowledgments

We thank Kun Gao and Chiung-Yin Chang for providing reviews of this paper. The simulations presented in this paper were performed using Stellar at Princeton University with help from the Princeton Institute for Computational Science and Engineering (PICSciE). This study is supported under awards NA18OAR4320123, NA19OAR0220146, and NA19OAR0220147 from the National Oceanic and Atmospheric Administration (NOAA), U.S. Department of Commerce. This project was additionally funded by the Weather Program Office, Office of Oceanic and Atmospheric Research, NOAA. Bretherton and Clark acknowledge funding from the Allen Institute for Artificial Intelligence. The statements, findings, conclusions, and recommendations are those of the authors and do not necessarily reflect the views of NOAA, or the U.S. Department of Commerce.

Open Research

SHiELD is available at https://github.com/NOAA-GFDL/SHiELD_build and described in detail by (Harris et al., 2020). Data presented in this study are available at https://doi.org/10.5281/zenodo.6585122.

References

Chen, J., Dai, A., Zhang, Y., & Rasmussen, K. L. (2020). Changes in Convective Available Potential Energy and Convective Inhibition under Global Warming. *Journal of Climate*, *33*(6), 2025–2050. https://doi.org/10.1175/JCLI-D-19-0461.1

Diffenbaugh, N. S., Scherer, M., & Trapp, R. J. (2013). Robust increases in severe thunderstorm environments in response to greenhouse forcing. *Proceedings of the National Academy of Sciences*, *110*(41), 16361–16366. https://doi.org/10.1073/pnas.1307758110

Eyring, V., Bony, S., Meehl, G. A., Senior, C. A., Stevens, B., Stouffer, R. J., & Taylor, K. E. (2016). Overview of the Coupled Model Intercomparison Project Phase 6 (CMIP6) experimental design and organization. *Geoscientific Model Development*, *9*(5), 1937–1958. https://doi.org/10.5194/gmd-9-1937-2016

Fasullo, J. (2012). A mechanism for land–ocean contrasts in global monsoon trends in a warming climate. *Climate Dynamics*, *39*(5), 1137-1147.

Han, J., Wang, W., Kwon, Y. C., Hong, S.-Y., Tallapragada, V., & Yang, F. (2017). Updates in the NCEP GFS Cumulus Convection Schemes with Scale and Aerosol Awareness. *Weather and Forecasting*, *32*(5), 2005–2017. https://doi.org/10.1175/WAF-D-17-0046.1

Harris, L., Zhou, L., Lin, S.-J., Chen, J.-H., Chen, X., Gao, K., et al. (2020). GFDL SHiELD: A Unified System for Weather-to-Seasonal Prediction. *Journal of Advances in Modeling Earth Systems*, *12*(10), e2020MS002223. https://doi.org/10.1029/2020MS002223

Harris, L., Chen, X., Putman, W., Zhou, L., & Chen, J.-H. (2021). A Scientific Description of the GFDL Finite-Volume Cubed-Sphere Dynamical Core. https://doi.org/10.25923/6nhs-5897

He, C., Zhou, T., Lin, A., Wu, B., Gu, D., Li, C., & Zheng, B. (2015). Enhanced or Weakened Western North Pacific Subtropical High under Global Warming? *Scientific Reports*, *5*(1), 16771. https://doi.org/10.1038/srep16771

He, J., Soden, B. J., & Kirtman, B. (2014). The robustness of the atmospheric circulation and precipitation response to future anthropogenic surface warming. *Geophysical Research Letters*, *41*(7), 2614-2622.

Houze Jr., R. A., Rasmussen, K. L., Zuluaga, M. D., & Brodzik, S. R. (2015). The variable nature of convection in the tropics and subtropics: A legacy of 16 years of the Tropical Rainfall Measuring Mission satellite. *Reviews of Geophysics*, *53*(3), 994–1021. https://doi.org/10.1002/2015RG000488

Judt, F., Klocke, D., Rios-Berrios, R., Vanniere, B., Ziemen, F., Auger, L., et al. (2021). Tropical Cyclones in Global Storm-Resolving Models. *Journal of the Meteorological Society of Japan. Ser. II*, *99*(3), 579–602. https://doi.org/10.2151/jmsj.2021-029

Lepore, C., Abernathey, R., Henderson, N., Allen, J. T., & Tippett, M. K. (2021). Future Global Convective Environments in CMIP6 Models. *Earth's Future*, *9*(12), e2021EF002277. https://doi.org/10.1029/2021EF002277

Liu, C., Zipser, E. J., & Nesbitt, S. W. (2007). Global Distribution of Tropical Deep Convection: Different Perspectives from TRMM Infrared and Radar Data. *Journal of Climate*, *20*(3), 489–503. https://doi.org/10.1175/JCLI4023.1

Ringer, M. A., Andrews, T., & Webb, M. J. (2014). Global-mean radiative feedbacks and forcing in atmosphere-only and coupled atmosphere-ocean climate change experiments. *Geophysical Research Letters*, *41*(11), 4035–4042. https://doi.org/10.1002/2014GL060347

Niu, G.-Y., Yang, Z.-L., Mitchell, K. E., Chen, F., Ek, M. B., Barlage, M., et al. (2011). The community Noah land surface model with multiparameterization options (Noah-MP): 1. Model description and evaluation with local-scale measurements. *Journal of Geophysical Research: Atmospheres*, *116*(D12). https://doi.org/10.1029/2010JD015139

Nugent, J. M., Turbeville, S. M., Bretherton, C. S., Blossey, P. N., & Ackerman, T. P. (2022). Tropical Cirrus in Global Storm-Resolving Models: 1. Role of Deep Convection. *Earth and Space Science*, *9*(2), e2021EA001965. https://doi.org/10.1029/2021EA001965

Pollard, R. T., Rhines, P. B., & Thompson, R. O. R. Y. (1973). The deepening of the wind-Mixed layer. *Geophysical Fluid Dynamics*, *4*(4), 381–404. https://doi.org/10.1080/03091927208236105

Putman, W. M., & Lin, S.-J. (2007). Finite-volume transport on various cubed-sphere grids. *Journal of Computational Physics*, *227*(1), 55–78. https://doi.org/10.1016/j.jcp.2007.07.022

Satoh, M., Stevens, B., Judt, F., Khairoutdinov, M., Lin, S.-J., Putman, W. M., & Düben, P. (2019). Global Cloud-Resolving Models. *Current Climate Change Reports*, *5*(3), 172–184. https://doi.org/10.1007/s40641-019-00131-0

Singh, M. S., & O'Gorman, P. A. (2015). Increases in moist-convective updraught velocities with warming in radiative-convective equilibrium. *Quarterly Journal of the Royal Meteorological Society*, *141*(692), 2828–2838. https://doi.org/10.1002/qj.2567

Sobel, A. H., & Camargo, S. J. (2011). Projected future seasonal changes in tropical summer climate. *Journal of Climate*, *24*(2), 473-487.

Stevens, B., Satoh, M., Auger, L., Biercamp, J., Bretherton, C. S., Chen, X., et al. (2019). DYAMOND: the DYnamics of the Atmospheric general circulation Modeled On Non-hydrostatic Domains. *Progress in Earth and Planetary Science*, *6*(1), 61. https://doi.org/10.1186/s40645-019-0304-z

Taszarek, M., Allen, J. T., Marchio, M., & Brooks, H. E. (2021). Global climatology and trends in convective environments from ERA5 and rawinsonde data. *Npj Climate and Atmospheric Science*, *4*(1), 1–11. https://doi.org/10.1038/s41612-021-00190-x

Taylor, K. E., Stouffer, R. J., & Meehl, G. A. (2012). An Overview of CMIP5 and the Experiment Design. *Bulletin of the American Meteorological Society*, *93*(4), 485–498. https://doi.org/10.1175/BAMS-D-11-00094.1

Tsushima, Y., Iga, S., Tomita, H., Satoh, M., Noda, A. T., & Webb, M. J. (2014). High cloud increase in a perturbed SST experiment with a global nonhydrostatic model including explicit convective processes. *Journal of Advances in Modeling Earth Systems*, *6*(3), 571–585. https://doi.org/10.1002/2013MS000301

Turbeville, S. M., Nugent, J. M., Ackerman, T. P., Bretherton, C. S., & Blossey, P. N. (2022). Tropical Cirrus in Global Storm-Resolving Models: 2. Cirrus Life Cycle and Top-of-Atmosphere Radiative Fluxes. *Earth and Space Science*, *9*(2), e2021EA001978. https://doi.org/10.1029/2021EA001978

Vecchi, G. A., & Soden, B. J. (2007). Global Warming and the Weakening of the Tropical Circulation. *Journal of Climate*, *20*(17), 4316–4340. https://doi.org/10.1175/JCLI4258.1

WMO. (2021). *WMO Atlas of Mortality and Economic Losses from Weather, Climate and Water Extremes (1970–2019) (WMO-No. 1267)*. Geneva: WMO.

Wyant, M. C., Bretherton, C. S., Bacmeister, J. T., Kiehl, J. T., Held, I. M., Zhao, M., et al. (2006). A comparison of low-latitude cloud properties and their response to climate change in three AGCMs sorted into regimes using mid-tropospheric vertical velocity. *Climate Dynamics*, *27*(2), 261–279. https://doi.org/10.1007/s00382-006-0138-4

Zhao, M. (2022). A Study of AR-, TS-, and MCS-Associated Precipitation and Extreme Precipitation in Present and Warmer Climates. *Journal of Climate*, *35*(2), 479–497. https://doi.org/10.1175/JCLI-D-21-0145.1

Zhou, L., Harris, L., Chen, J.-H., Gao, K., Guo, H., Xiang, B., et al. (2022). Weather Prediction in SHiELD: Effect from GFDL Cloud Microphysics Scheme Upgrade. *Earth and Space Science Open Archive*, 30. https://doi.org/10.1002/essoar.10510017.1

Zhou, T., Yu, R., Zhang, J., Drange, H., Cassou, C., Deser, C., et al. (2009). Why the Western Pacific Subtropical High Has Extended Westward since the Late 1970s. *Journal of Climate*, *22*(8), 2199–2215. https://doi.org/10.1175/2008JCLI2527.1